# EOS Microwave Limb Sounder observations of upper stratospheric BrO: Implications for total bromine

Nathaniel J. Livesey[1], Laurie J. Kovalenko[2,1], Ross J. Salawitch[1], Ian A. MacKenzie[3],

Martyn P. Chipperfield[4], William G. Read[1], Robert F. Jarnot[1] and Joe W. Waters[1]

Short title:

[1]Jet Propulsion Laboratory, California Institute of Technology

[2]Columbus Technologies and Services Inc.

[3]University of Edinburgh

[4]Institute of Atmospheric Science, School of Earth and Environment, University of Leeds

**Abstract.** This paper describes new total stratospheric inorganic bromine ($Br_y$) abundance estimates infered from the first global observations of upper stratospheric BrO, made by the EOS Microwave Limb Sounder on the Aura satellite. Our 'best estimate' of total upper stratospheric bromine loading (based on JPL-2002 kinetics with the addition of a $BrONO_2 + O$ reaction) is $18.6 \pm 5$ pptv, for the period September 2004 to August 2005. This implies a contribution of $3.0 \pm 5$ pptv from sources other than long lived $CH_3Br$ and halons. The possibility of such other sources has been raised by balloon, aircraft and satellite observations of BrO in the lower and middle stratosphere. These upper stratospheric observations provide new information to help resolve the current uncertainty in stratospheric bromine loading. The abundance of bromine, particularly in the lower stratosphere, is a significant factor in the budgets of stratospheric $O_3$.

## Introduction

Stratospheric bromine and its role in photochemical $O_3$ destruction have received much attention in recent studies [e.g., *Salawitch et al.*, 2005]. Estimates of total stratospheric bromine loading based on observations of stratospheric BrO generally indicate 4 – 6 pptv more bromine than would be expected from contributions of the known long-lived source gases $CH_3Br$ and halons [*WMO*, 2003]. This excess in total inorganic bromine ($Br_y$) may reflect the contributions of short-lived halogenated species in the stratosphere [e.g., *Wamsley et al.*, 1998; *Pfeilsticker et al.*, 2000], or of upper tropospheric BrO transported into the stratosphere [*Pfeilsticker et al.*, 2000]. Either scenario implies larger abundances of reactive bromine in the lower stratosphere than is often assumed in model simulations of $O_3$ chemistry. In this region, where the bulk of the chlorine is still in non-reactive organic forms, bromine plays a more significant role in photochemical $O_3$ destruction than elsewhere, and the rate of $O_3$ loss is very sensitive to the amount of inorganic bromine. [*WMO*, 2003; *Salawitch et al.*, 2005].

Here we present new global observations of upper stratospheric BrO from the Microwave Limb Sounder (MLS) on Aura [*Waters et al.*, 2006], which are used in conjunction with models to infer the total upper stratospheric bromine loading.

## MLS BrO observations

**Figure 1.**

The MLS instrument on the EOS Aura spacecraft, launched in July 2004, observes two sets of BrO thermal emission lines in the 640 GHz region. Figure 1 shows observations from one of these sets. The 2 – 3 K noise on individual limb radiance measurements is

very large compared to the typically 0.1 – 0.2 K spectral signature of BrO. Accordingly, significant averaging is required to obtain BrO abundance estimates with a scientifically useful signal-to-noise ratio.

The version 1.51 of the MLS data processing algorithms [*Livesey et al.*, 2006], the first MLS data version released for public use, produces ∼3500 BrO abundance profiles daily with a typical precision of 200 – 300 pptv. When averages such as monthly zonal means are taken of this product, large amounts of noise are still seen in the data, due to a poor choice made in the v1.51 configuration in the tradeoff between precision and vertical resolution.

For this study, an 'off-line' BrO algorithm has been developed which produces a pair of zonal mean abundance fields (as a function of pressure and latitude) for each day, one for the ascending (mostly daytime) part of the orbit, the other for descending (mostly nighttime). These are retrieved from 10°-latitude-resolution zonal averages of the daily radiance observations. The daily zonal mean BrO abundances retrieved have an estimated precision of 10 – 20 pptv in the mid- and upper stratosphere. Seasonal averaging of these gives abundances with a precision of ∼2 pptv which is useful in comparison to the 10 – 15 pptv typical abundance of BrO.

**Figure 2.**

Figure 2 shows seasonal zonal means of the ascending (a) and descending (b) MLS BrO. These show the generally expected behavior, with ∼9 – 15 pptv of BrO seen in much of the upper stratosphere during daytime and essentially zero BrO at night. Lower average BrO abundances are seen in polar night regions on the ascending side of the orbit while significant abundance is seen in the polar day side on the descending half. The descending (mainly nighttime) abundances are somewhat unrealistically large around 10 hPa (larger still at greater

pressures not shown). These are indicative of biases in the data (essentially zero BrO is expected at night in these regions). These biases are mainly due to inaccuracies in the retrieval method which become more significant with increasing pressure as line-broadening increases the contribution of other molecules to the MLS radiances in the BrO spectral region. Taking day/night differences in the retrieved BrO in the regions where the nighttime abundances are known a priori to be negligible (at pressures greater than 3 hPa) alleviates some of this bias. Figure 2c shows this difference for altitudes below the 3.16 hPa MLS pressure surface. In the low and mid-latitudes the bias has been alleviated. However, in polar regions, the ascending and descending orbital phases are often both day (polar summer) or night (polar winter), so differences in these regions are not useful measures of the daytime BrO abundance.

For the purposes of this study, we consider latitudes between 55°S and 55°N, using ascending/descending differences as a measure of daytime BrO for pressures greater than the 3.16 hPa MLS surface and ascending observations only for 3.16 hPa and lesser pressures.

**Accuracy assessment for the off-line BrO product**

The accuracy of this off-line BrO product is dependent on knowledge of instrument calibration and spectroscopy, and also on the performance of the retrieval algorithm. Instrument calibration and spectroscopic uncertainties are estimated to give respectively a $10-20\%$ and $3\%$ uncertainty in the BrO product.

The accuracy of the retrieval algorithm is estimated by two independent techniques. Firstly, we take advantage of the fact that the off-line algorithms also retrieve $O_3$ and $HNO_3$ abundances that are based on observations of weak emission lines of these molecules (actually

various excited states and isotopomers) in the vicinity of the BrO lines. One measure of the accuracy of the off-line algorithms is therefore the level of agreement between these products and the well understood $O_3$ and $HNO_3$ products produced by the version 1.51 algorithms which use stronger lines from these species. Secondly, the off-line product is based on a linearized forward model [*Read et al.*, 2006]. The accuracy of this approach can be quantified by running a retrieval with the radiances all set to zero. The departure of the resulting BrO from the expected zero abundance is another measure of the BrO accuracy.

**Figure 3.**

We estimate the overall accuracy of the BrO product (shown in Figure 3) as the root sum of the squares of the 20% calibration and 3% spectroscopic uncertainties and the overall retrieval accuracy. The latter is defined as the worst accuracy at each level obtained from the three independent estimates ($O_3$, $HNO_3$ and zero radiance).

Previous balloon observations of BrO [*Pfeilsticker et al.*, 2000; *Pundt et al.*, 2002] do not reach the altitudes considered here, and so direct comparisons with these for validation purposes is not possible.

## Using models to infer total bromine

BrO is the dominant form of bromine in the daytime upper stratosphere, accounting for ~60% of the total bromine loading. Model calculations are used to infer the total stratospheric bromine abundance, needed to asses the impact of bromine on stratospheric $O_3$. We use two approaches, based on different models.

**The SLIMCAT model**

For our analysis, the SLIMCAT model [*Chipperfield*, 1999] is run in 'near-real time' driven by U.K. Met Office analysis fields. Model fields are sampled at the same locations and times (to the nearest 30 minute time step) of the MLS profile observations. By sampling the model in this manner, the diurnal cycle of BrO is fully accounted for. The SLIMCAT model is used to infer the total inorganic bromine abundance corresponding to the MLS observation according to

$$\mathrm{Br_y}^{\mathrm{MLS}} = \mathrm{BrO}^{\mathrm{MLS}} \left( \frac{\mathrm{Br_y}^{\mathrm{SLIMCAT}}}{\mathrm{BrO}^{\mathrm{SLIMCAT}}} \right). \quad (1)$$

This run of the SLIMCAT model has been initialized with 16 pptv $CH_3Br$ and 6 pptv of inorganic bromine (representing short lived sources) at the 326 K model boundary. The model shows all of the bromine in inorganic form at pressures smaller than 30 hPa. SLIMCAT predicts unrealistically large abundances of BrO in the night-time upper stratosphere (3 hPa and lesser pressures) due to assuming steady state for $HO_x$ species whose abundances therefore become near-zero just after sunset, preventing formation of, e.g., HOBr. Details of the reactions and rates used in both SLIMCAT and our other model are given below.

The calculation in (1) is performed for the daily zonal means of BrO and $Br_y$ from SLIMCAT and daily zonal mean BrO from MLS (ascending and ascending/descending difference, as described above). The resulting daily zonal mean $Br_y$ abundances are further averaged to increase the signal-to-noise ratio.

**The photochemical diurnal-steady-state box model**

In addition to SLIMCAT, a constrained diurnal photochemical steady-state model [*Osterman et al.*, 1997] (PSS hereafter) is used to infer total bromine abundance from the MLS BrO observations. This method was used similarly in *Sioris et al.* [2006]. This model is constrained to MLS observations of temperature, $O_3$ and water vapor, and also to an $NO_y$ abundance inferred from MLS $N_2O$ observations using well established tracer relations [*Popp et al.*, 2001; *Rinsland et al.*, 1996]. The total bromine loading is treated as a free parameter that is iteratively adjusted until the modeled BrO abundance matches the MLS observations. We ran the model with two sets of kinetics parameters. In one case, which we call JPL02, we used JPL-2002 kinetics [*Sander et al.*, 2003]; in the other, which we call JPL02a, we added the reaction [*Soller et al.*, 2001]

$$\mathrm{BrONO_2} + \mathrm{O} \rightarrow \mathrm{BrO} + \mathrm{NO_3}. \tag{2}$$

While not in the JPL-2002 kinetics compendium, this reaction is expected to have a large effect on stratospheric bromine partitioning [*Soller et al.*, 2001; *Sinnhuber et al.*, 2002] and is used in the SLIMCAT model configuration described above.

As with the SLIMCAT calculation, the PSS model is run for the daily zonal mean MLS BrO. The resulting daily $Br_y$ zonal means are averaged together to increase the signal-to-noise ratio. As the daily zonal mean MLS BrO abundances are noisy, negative values occur, which cannot be handled by the PSS model. Ignoring these would give a positive bias in averages subsequently computed. Instead the sign is reversed both on the BrO input to PSS (to make it positive) and on the resulting $Br_y$ (back to negative) before averaging.

**Comparison of inferred $Br_y$ for two models**

**Figure 4.**

Figure 4 shows values of $Br_y$ estimated by these two models in the form of averages for four seasons (the PSS model run shown uses JPL02a kinetics). Little difference in $Br_y$ is expected from season to season, so significant variations would indicate stability problems with the MLS BrO observations or with the models used to infer $Br_y$. The $Br_y$ abundances agree from season to season to within what is expected from the precision of the MLS BrO observations (red error bars). There is, however, a notable disagreement between the two models, with SLIMCAT inferring $\sim$2 pptv more $Br_y$ than PSS.

This disagreement is mainly due to differences in the model abundances of $O_3$ and $NO_y$. SLIMCAT computes its own values of these, while PSS uses MLS observations for $O_3$ and $NO_y$ abundances inferred from MLS $N_2O$. When PSS is run using SLIMCAT estimates of $O_3$ and $NO_y$ and constrained to SLIMCAT BrO, it infers $Br_y$ that matches SLIMCAT's assumed 22 pptv Bry abundance to within $\pm$0.6 pptv.

**Figure 5.**

Figure 5a compares the vertical profiles of $O_3$ used in the two models (i.e., SLIMCAT's calculation and MLS observations). These profiles are an average over 55°S to 55°N for one year. In the 10 to 2.2 hPa altitude range relevant here, SLIMCAT $O_3$ is consistently lower than MLS observations (averages over shorter times show the same result). The lower $O_3$ abundance in SLIMCAT lowers the production rate of BrO via the reactions $HOBr + O \rightarrow BrO + OH$ and $BrONO_2 + O \rightarrow BrO + NO_3$, which in turn lowers the $BrO/Br_y$ ratio, increasing the value of $Br_y$ inferred from MLS BrO. In this altitude region, the MLS $O_3$ measurements have been shown to agree within 10% with other observations [*Froidevaux*

*et al.*, 2006]. The $O_3$ deficit seen in the SLIMCAT model is well-known [e.g., *Osterman et al.*, 1997], although here it is occurring at altitudes lower than expected.

Similarly, there is a systematic difference between the $NO_y$ abundances in the two models, with SLIMCAT consistently showing more $NO_y$ than inferred from MLS measurements of $N_2O$. Although there are no independent measurements of $NO_y$ that we can directly compare with, there are sunrise and sunset $NO_2$ data from the Halogen Occultation Experiment (HALOE) [*Gordley et al.*, 1996] on board the Upper Atmosphere Research Satellite, which measured $NO_2$ profiles by infrared solar occultation. Figure 5b compares HALOE data (version 19) with sunset $NO_2$ produced by the PSS model using tracer-relation-inferred $NO_y$ from MLS $N_2O$, and with sunset $NO_2$ estimated from SLIMCAT $NO_y$ using the PSS model. SLIMCAT clearly overestimates the abundance of $NO_y$ in this region. The higher $NO_2$ in SLIMCAT increases the loss rate of BrO via the reactions $BrO + NO_2 + M \rightarrow BrONO_2 + M$, which in turn lowers the $BrO/Br_y$ ratio, again increasing the value of $Br_y$ inferred from MLS BrO.

## Results and discussions

**Figure 6.**

Figure 6 shows average $Br_y$ profiles obtained using PSS (JPL02 and JPL02a cases) and SLIMCAT. These have been averaged over one year of MLS measurements, from 55°S to 55°N. Further averaging over the MLS pressure surfaces from 10 hPa to 2.2 hPa gives estimates of 20.7 pptv from SLIMCAT and 19.2 and 18.6 pptv from PSS for the JPL02 and JPL02a cases, respectively. All three values are estimated to be accurate to ±5 pptv. Of the three, the JPL02a case (18.6 pptv) is considered the most accurate as it is based on the most

realistic atmospheric abundances of $O_3$ and $NO_y$ and the most up-to-date reaction rates. The large uncertainty in our results reflects the estimated accuracy of the MLS BrO product. Future versions of the MLS data processing algorithms should improve this accuracy.

From MLS measurements of $N_2O$ we estimate the year of stratospheric entry [*Engel et al.*, 2002] of the air sampled in this study to be 2000. Tropospheric methyl bromide and halons are estimated to have contributed 15.6 pptv total bromine at that time [*Montzka et al.*, 2003]. This estimate, based on a global average of tropospheric measurements of these gases obtained over the year 2000, accounts for a 7% loss of methyl bromide in the troposphere, and thus provides a lower limit. A second estimate of 17.0 pptv, based on projections from older data [*WMO*, 2003], does not account for any tropospheric loss of methyl bromide, and thus provides an upper limit. From the Montzka estimate, which is based on more recent data, our measurements imply 3.0±5 pptv of additional stratospheric bromine from other sources.

This compares well with estimates of 3±3 pptv obtained from SCIAMACHY observations [*Sinnhuber et al.*, 2005], though not so well with another estimate of 8.4±2 pptv, also from SCIAMACHY data [*Sioris et al.*, 2006]. Our observations are at the lower range of the estimates given by *Pfeilsticker et al.* [2000] and *Salawitch et al.* [2005], based on their analyses of aircraft and balloon data. Our results suggest a possible modest contribution of 3.0±5 pptv from VSL bromocarbons to the stratospheric bromine budget.

**Acknowledgments.** The research described in this paper carried out by the Jet Propulsion Laboratory, California Institute of Technology, under a contract with the National Aeronautics and Space Administration.

## References

Chipperfield, M. P. (1999), Multiannual simulations with a three-dimensional chemical transport model, *J. Geophys. Res.*, *104*, 1781–1805.

Engel, A., et al. (2002), Temporal development of total chlorine in the high-latitude stratosphere based on reference distributions of mean age derived from $CO_2$ and $SF_6$, *J. Geophys. Res.*, *107*(D12), 4136.

Froidevaux, L., et al. (2006), Early validation analyses of atmospheric profiles from EOS MLS on the Aura satellite, *IEEE Trans. Geosci. Remote Sens.*, *44*(5), 1106–1121.

Gordley, L. L., et al. (1996), Validation of nitric oxide and nitrogen dioxide measurements made by the Halogen Occultation Experiment for the UARS platform, *J. Geophys. Res.*, *101*(10,241–10,266).

Livesey, N. J., W. V. Snyder, W. G. Read, and P. A. Wagner (2006), Retrieval algorithms for the EOS Microwave Limb Sounder (MLS), *IEEE Trans. Geosci. Remote Sens.*, *44*(5), 1144–1155.

Montzka, S. A., J. H. Butler, B. D. Hall, D. J. Mondeel, and J. W. Elkins (2003), A decline in tropospheric organic bromine, *Geophys. Res. Lett.*, *30*(15), 1826, doi:10.1029/2003GL017745.

Osterman, G. B., R. J. Salawitch, B. Sen, G. C. Toon, R. A. Stachnik, H. M. Pickett, J. J. Margitan, J. F. Blavier, and D. B. Peterson (1997), Balloon-borne measurements of stratospheric radicals and their precursors: Implications for the production and loss of ozone, *Geophys. Res. Lett.*, *29*(9), 1107–1110.

Pfeilsticker, K., et al. (2000), Lower stratospheric organic and inorganic bromine budget for the Arctic winter 1998/99, *Geophys. Res. Lett.*, *27*(20), 3305–3308.

Popp, P. J., et al. (2001), Severe and extensive denitrification in the 1999–2000 Arctic winter stratosphere, *Geophys. Res. Lett.*, *28*(15), 2875–2878, doi:10.1029/2001GL013132.

Pundt, I., J. P. Pommereau, M. P. Chipperfield, M. V. Roozendael, and F. Goutail (2002), Climatology of the stratospheric BrO vertical distribution by balloon-borne UV–visible spectrometry, *J. Geophys. Res.*, *107*(D4), 4806, doi:10.1029/2002JD002230.

Read, W. G., Z. Shippony, M. J. Schwartz, N. J. Livesey, and W. V. Snyder (2006), The clear-sky unpolarized forward model for the EOS Microwave Limb Sounder (MLS), *IEEE Trans. Geosci. Remote Sens.*, *44*(5), 1367–1379.

Rinsland, C. P., et al. (1996), ATMOS meaurements of $H_2O$+2$CH_4$ and total reactive nitrogen in the November 1994 Antarctic stratosphere: Dehydration and denitrification in the vortex, *Geophys. Res. Lett.*, *23*(17), 2397, doi:10.1029/96GL00048.

Salawitch, R. J., et al. (2005), Sensitivity of ozone to bromine in the lower stratosphere, *Geophys. Res. Lett.*, *32*, L05,811, 10.1029/2004GL021504.

Sander, S. P., et al. (2003), Chemical kinetics and photochemical data for use in atmospheric studies, evaluation number 14, *Tech. rep.*, Jet Propulsion Laboratory, Pasadena, CA.

Sinnhuber, B. M., et al. (2002), Comparison of measurements and model calculations of stratospheric bromine monoxide, *J. Geophys. Res.*, *107*(D19), 4398, doi:10.1029/2001JD000940.

Sinnhuber, B. M., et al. (2005), Global observations of stratospheric bromine monoxide from SCIAMACHY, *Geophys. Res. Lett.*, *23*, L20,810, doi:10.1029/2005GL023839.

Sioris, C. E., et al. (2006), Latitudinal and vertical distribution of bromine monoxide in the lower stratosphere from SCIAMACHY limb scattering measurements, *J. Geophys. Res.*, in press.

Soller, R., J. M. Nicovich, and P. H. Wine (2001), Temperature-dependent rate coefficients for the reactions of $Br(^2P_{3/2})$, $Cl(^2P_{3/2})$ and $O(^3P_J)$ with $BrONO_2$, *J. Phys. Chem. A*, *105*, 1416–1422.

Wamsley, P. R., et al. (1998), Distribution of halon-1211 in the upper troposphere and lower stratosphere and the 1994 total bromine budget, *J. Geophys. Res.*, *103*(D1), 1513–1526.

Waters, J. W., et al. (2006), The Earth Observing System Microwave Limb Sounder (EOS MLS) on the Aura satellite, *IEEE Trans. Geosci. Remote Sens.*, *44*(5), 1075–1092.

WMO (2003), World meteorological organization, scientifc assessment of ozone depletion, *Tech. rep.*, World Meteorological Organization, Geneva Switzerland.

Received _____

This manuscript was prepared with AGU's LaTeX macros v5, with the extension package 'AGU$^{++}$' by P. W. Daly, version 1.6b from 1999/08/19.

## Figure Captions

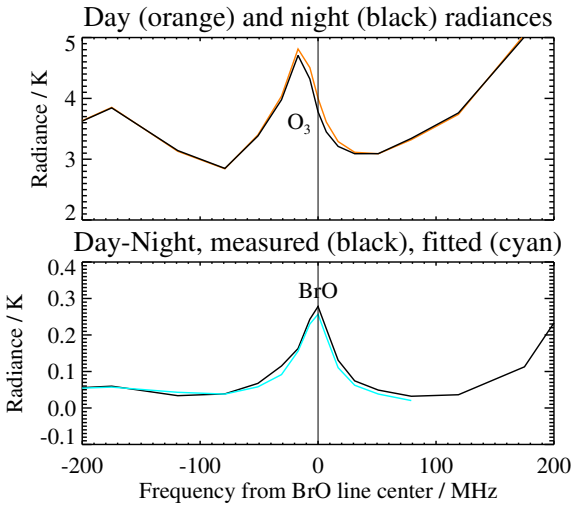


**Figure 1.** Top: average upper stratospheric MLS radiances observed in the region of the 650.19 GHz BrO lines. Black line is radiances measured during the descending (nighttime) part of the Aura orbit, orange is ascending (daytime). Average is from 55°S to 55°N, for limb rays with tangent pressures between ∼10 hPa and 3.3 hPa, for the period September 2004 to August 2005. The emission signature of an isotopic $O_3$ line is indicated. Bottom: difference between day and night measured radiances (black). The BrO spectral signature is clearly seen, due to the strongly diurnal nature of BrO at these altitudes. Cyan line shows the fit achieved to this signal by the retrieval algorithm described in the text.

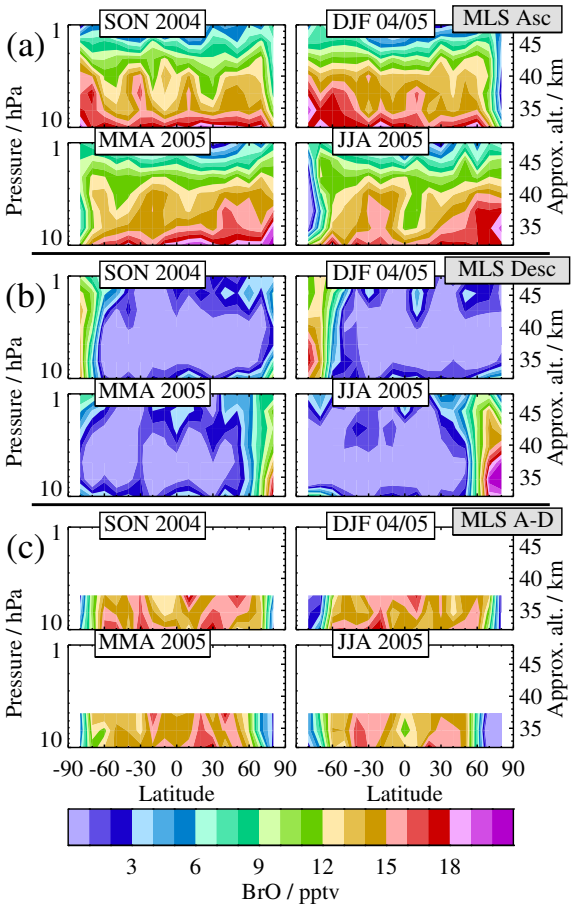


**Figure 2.** Seasonal zonal means of MLS BrO observations from (a) the ascending (mainly daytime) and (b) descending (mainly nighttime) phases of the orbits. The precision on these averages is 1–2 pptv over the vertical range shown. To alleviate biases in the lower regions, the difference (c) between ascending and descending can be used as a measure of daytime BrO at low and mid-latitudes, so long as the nighttime abundance of BrO is negligible, which is the case for pressures greater than 3 hPa.

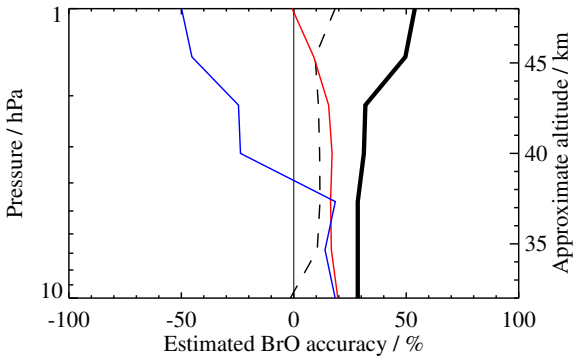


**Figure 3.** The estimated accuracy of the off-line BrO product. The red and blue lines show the estimates inferred from study of the offline $O_3$ and $HNO_3$ products, respectively. The dashed line shows the accuracy predicted from retrievals of zero radiance. The heavy black line shows the overall accuracy estimate, including the 3% spectroscopy and 20% calibration contributions.

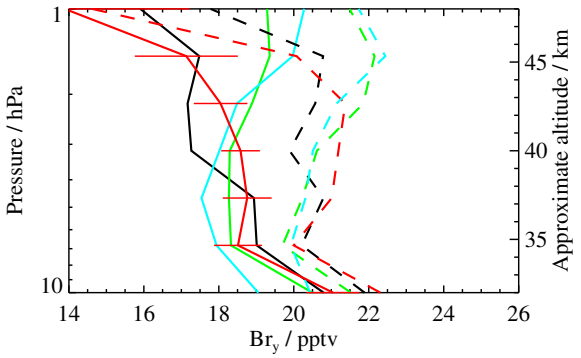


**Figure 4.** Seasonal average (from 55°S to 55°N) of $Br_y$ estimated by the PSS (solid) and SLIMCAT (dashed) models. Black, red, green and blue, respectively, indicate the same four seasons shown in Figure 2. The error bars on the D/J/F 2004/2005 SLIMCAT line (red) show the precision of the estimated $Br_y$ (due to radiance noise on MLS BrO), representative of all the lines.

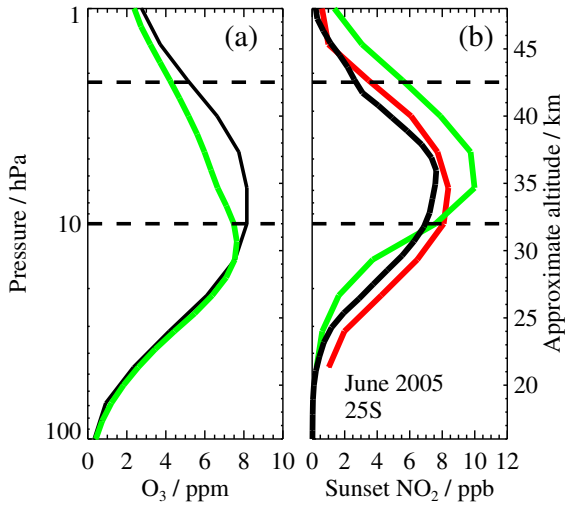


**Figure 5.** Comparison of vertical profiles of (a) $O_3$ and (b) $NO_2$ for the two models. The two dashed horizontal lines bracket the altitude region relevant to this work. In (a), SLIMCAT model $O_3$ isgreen, MLS data, used as input for the PSS model, is black. The profiles are a yearly average from 55°N to 55°S. For altitudes relevant to this study, SLIMCAT model $O_3$ is consistently lower than MLS measurements. In (b), sunset $NO_2$ is shown for both models (SLIMCAT green, PSS red) and compared with HALOE data (black). For most latitudes and seasons, in the altitude region relevant to this work, PSS model $NO_2$ is consistently lower than SLIMCAT, in better agreement with HALOE data.

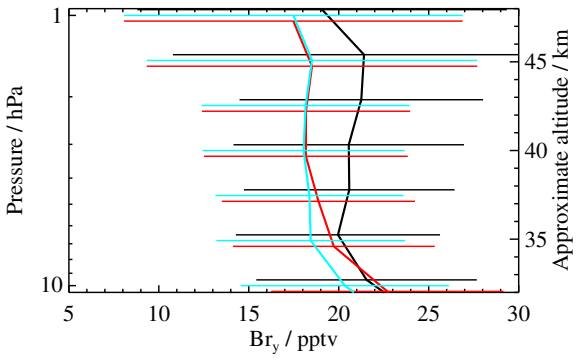


**Figure 6.** Average $Br_y$ inferred from MLS data using the SLIMCAT (black) and PSS models (red with JPL02 kinetics, cyan with JPL02a). Average is from September 2004 through August 2005, over latitudes from 55°S to 55°N. Error bars reflect the accuracy of the underlying MLS BrO.